Cooperative regulation of C1-domain membrane recruitment polarizes atypical Protein Kinase C

Kimberly A. Jones*, Michael L. Drummond*, and Kenneth E. Prehoda

Institute of Molecular Biology
Department of Chemistry and Biochemistry
1229 University of Oregon
Eugene, OR 97403

*Equal contributions

Corresponding author: prehoda@uoregon.edu

Abstract

Recruitment of the Par complex protein atypical Protein Kinase C (aPKC) to a specific membrane domain is a key step in the polarization of animal cells. While numerous proteins and phospholipids interact with aPKC, how these interactions cooperate to control its membrane recruitment has been unknown. Here we identify aPKC's C1 domain as a phospholipid interaction module that targets aPKC to the membrane of *Drosophila* neural stem cells (NSCs). The isolated C1 binds the NSC membrane in an unpolarized manner during interphase and mitosis and is uniquely sufficient among aPKC domains for targeting. Other domains, including the catalytic module and those that bind the upstream regulators Par-6 and Baz, restrict C1's membrane targeting activity spatially and temporally – to the apical NSC membrane during mitosis. Our results suggest that Par complex polarity results from cooperative activation of autoinhibited C1 membrane binding activity.

Introduction

The Par complex polarizes animal cells by excluding specific cortical factors from the Par cortical domain (Lang and Munro, 2017; Venkei and Yamashita, 2018). During polarization the Par complex, consisting of Par-6 and atypical Protein Kinase C (aPKC), is recruited to a specific, continuous region of the cell membrane such as the apical surface of epithelia (Tepass, 2012), the anterior hemisphere of the *C. elegans* zygote (Nance and Zallen, 2011), or the apical hemisphere of *Drosophila* neural stem cells (NSCs) (Prehoda, 2009). Factors that are polarized by the Par complex, such as Miranda and Numb, are aPKC substrates (Atwood and Prehoda, 2009; Smith et al., 2007). Phosphorylation is coupled to removal from the Par domain, causing these substrates to form a complementary membrane domain (Bailey and Prehoda, 2015). Thus, the pattern of Par-polarized factors is ultimately determined by the mechanisms that specify aPKC's membrane recruitment and activation.

Many aPKC interactions with proteins and phospholipids have been identified (Figure 1A), although how they collaborate to polarize aPKC remains poorly understood. Bazooka (Baz aka Par-3) and Par-6 form direct physical contacts with aPKC and each protein has possible pathways for membrane recruitment, Baz through direct interactions with the membrane and Par-6 through interactions with prenylated Cdc42 (Joberty et al., 2000; Lin et al., 2000; Krahn et al., 2010). Several direct interactions with phospholipids have also been reported, including with ceramide (Wang et al., 2005), sphingosine 1-phosphate (Kajimoto et al., 2019), and the phosphoinositides PI (4,5)P_2, and PI (3,4,5)-P_3 (Standaert et al., 1997). The aPKC catalytic

domain may also play a role in membrane recruitment as perturbations in this domain can cause aPKC to become depolarized (i.e. localized uniformly to the membrane) (Rodriguez et al., 2017; Hannaford et al., 2019).

While interactions that could potentially recruit aPKC to the membrane have been identified, what is missing is an understanding of how the interactions function together to yield aPKC polarity. One possibility is that each interaction is weak, unable to recruit aPKC to the membrane on its own, but the energy provided by multiple weak interactions allows for recruitment (i.e. avidity). Alternately, one or more interactions could be responsible for recruitment but somehow regulated to ensure that targeting only occurs when the appropriate cues are present. These models could be distinguished by determining if any interactions lead to constitutive membrane recruitment (i.e. if one or more domains were sufficient for targeting).

We used *Drosophila* NSCs to investigate how aPKC is recruited to the membrane during polarization (Homem and Knoblich, 2012). During NSC interphase, aPKC is cytoplasmic but becomes targeted to the apical hemisphere early in mitosis, ultimately concentrating near the apical pole before depolarizing and returning to the cytoplasm as division completes (Oon and Prehoda, 2019). The highly dynamic nature of the NSC polarity cycle makes it possible to assess both spatial (polarized, depolarized, or cytoplasmic) and temporal (interphase or mitotic) aspects of aPKC membrane recruitment regulation.

Results

Mutations that inactivate catalytic activity depolarize aPKC

We began our examination of aPKC membrane targeting mechanisms in NSCs by evaluating the role of the catalytic domain. At metaphase, aPKC is highly enriched at the apical membrane of larval brain NSCs (Rolls et al., 2003). We examined the effect of mutations that inactivate aPKC's catalytic activity on its localization in cells that lacked endogenous aPKC (*apkc*^{K06403} in positively marked clones; Lee and Luo, 1999). Besides aPKC's localization, we also examined its activity in these NSCs by determining the localization of Miranda (Mira), an aPKC substrate that is normally restricted to the basal cortex by apical aPKC activity (Figure 1B) (Atwood and Prehoda, 2009; Ikeshima-Kataoka et al., 1997). Consistent with previous observations, we found that in metaphase *apkc*^{K06403} NSCs, Mira was allowed to enter the apical cortex becoming uniformly cortical (Figure 1B). Furthermore, expression of wild-type

63 aPKC restored the apical aPKC and basal Mira localization found in normally functioning NSCs
64 to *aPKC*^{K06403} null clones (Figure 1B, Holly et al., 2020).

65 To examine the effect of perturbing catalytic activity, we expressed aPKC harboring a mutation
66 (D388A) that does not have detectable activity in an *in vitro* protein kinase assay (Holly et al.,
67 2019). This mutation is in a residue that coordinates the γ-phosphate of ATP and is thought to
68 prevent phosphotransfer while allowing ATP to bind (Cameron et al., 2009). Unlike wild-type
69 aPKC, which is restricted to the apical domain at metaphase, we found that aPKC D388A was
70 largely depolarized, localizing to the entire cortex of *aPKC*^{K06403} metaphase null clones (Figure
71 1A). Mira also localized uniformly to the cortex in these cells, confirming that aPKC D388A is
72 inactive both *in vitro* (Holly et al., 2019) and *in vivo* (Figure 1B-F). Interestingly, the kinase
73 inactivating mutation also caused aPKC to associate with the membrane during interphase, a
74 cell cycle period in which it is normally cytoplasmic (Figure 1D,F). We conclude that inactivation
75 of the aPKC catalytic domain causes aPKC to constitutively localize to the membrane.

76 **Kinase inactive aPKC's localization is not restored by endogenous aPKC**

77 Our results indicate that mutations that perturb aPKC's catalytic activity also influence its
78 localization, both spatially and temporally, leading to constitutive depolarization. Previous
79 observations using chemically inhibited aPKC also found that perturbations to catalytic activity
80 caused depolarization (Rodriguez et al., 2017; Hannaford et al., 2019). The depolarization
81 caused by perturbations to the kinase domain could be explained if aPKC's catalytic activity
82 directly participated in its own localization (e.g. by activating an upstream regulator via
83 phosphorylation). Alternately, however, perturbations in the kinase domain could alter other
84 aPKC functions. Besides catalyzing phosphotransfer, the aPKC kinase domain also binds a
85 pseudosubstrate in its NH_2-terminal region causing autoinhibition (Graybill et al., 2012).
86 Mutations or small molecules that influence the active site could perturb the intramolecular
87 interaction in addition to inhibiting catalytic activity. To determine whether the loss of aPKC's
88 catalytic activity is responsible for the localization defects of D388A aPKC, we determined
89 whether the presence of wild-type, endogenous aPKC with its normal level of catalytic activity
90 could restore aPKC D388A polarity. We also tested the localization of a well-studied kinase
91 inactive mutation K293W, which blocks ATP binding (Graybill et al, 2012). In NSCs containing
92 endogenous aPKC, both aPKC D388A and K293W remained depolarized indicating that aPKC
93 catalytic activity is not sufficient to restore polarity to these proteins. Interestingly, in cells
94 expressing aPKC K293W Mira polarity was restored, confirming that aPKC activity was

95 present, but in cells expressing aPKC D388A, Mira remained depolarized suggesting that aPKC
96 D388A influences the localization or activity of endogenous aPKC (Figure 1C).

97 We also examined whether kinase inactive aPKC mutants influence the localization of Baz or
98 Par-6, proteins that directly interact with aPKC. We found that Baz remained apically polarized
99 in cells expressing aPKC, as well as those expressing the aPKC D388A or aPKC K293W
100 variants, although the intensity of this crescent was slightly reduced in aPKC D388A (Figure 2A,
101 C). While Baz localization was unperturbed by the expression of the kinase inactive aPKC
102 variants, Par-6 expanded into the basal domain like the localization of aPKC D388A and aPKC
103 K293W (Figure 2A, B). This pattern of localization is similar to that of an analog sensitive variant
104 of aPKC that also caused depolarization of Par-6 but not Baz (Hannaford et al., 2019). We
105 conclude that expression of kinase inactive aPKC leads to loss of Par-6 polarity but does not
106 influence the localization of Baz.

107 **Kinase inactive aPKC binds the NSC membrane independent of Cdc42 and Bazooka**
108 Membrane targeting of aPKC normally requires the activity of Baz and the small GTPase
109 Cdc42 (Wodarz et al., 2000; Rolls et al., 2003; Atwood et al., 2007). We tested whether these
110 upstream regulators are required for the uniformly cortical localization of kinase inactive aPKC
111 by examining the localization of aPKC K293W in NSCs expressing Baz or Cdc42 RNAi. We
112 found that wild-type aPKC failed to recruit to the membrane in these contexts, as previously
113 reported (Figure 3A-D) (Atwood et al., 2007; Rolls et al., 2003). Consistent with this
114 observation, we found that Mira was depolarized, localizing uniformly to the cortex in these
115 cells. In contrast to wild-type aPKC, however, aPKC K293W was able to remain on the cortex
116 even when Cdc42 was absent (Figure 3A-B). We also examined the localization of aPKC and
117 the K293W variant in NSCs expressing Baz RNAi. In this context, wild-type aPKC appears
118 more cytoplasmic and Mira becomes depolarized as expected (Atwood et al., 2007). Like
119 NSCs expressing Cdc42 RNAi, however, aPKC K293W's cortical localization was not affected
120 when Baz was reduced (Figure 3C-D). We conclude that aPKC K293W does not rely on Cdc42
121 or Baz for cortical targeting.

122 **The aPKC C1 domain is a constitutive membrane targeting module**
123 Our results indicate that the uniform membrane localization of aPKC with inactive kinase
124 domains (e.g. K293W) is independent of both Baz and Cdc42. One model consistent with
125 these results is that aPKC contains a membrane targeting module that is regulated by its

126 kinase domain, Baz, and Cdc42. To identify the putative module, we first examined whether
127 removing the kinase domain leads to the same uniform membrane localization phenotype. As
128 shown in Figure 4B, D-E, aPKC PB1-C1 (i.e. ΔKD) was uniformly localized in NSCs. A similar
129 localization pattern has been reported for aPKC PB1-C1 expressed in cultured cells (Dong et
130 al., 2020). Thus, aPKC's NH_2-terminal regulatory region contains the domain responsible for
131 membrane binding. The regulatory region has three domains, PB1, PS and C1, each of which
132 has the potential to interact with the membrane. The PB1 could mediate interaction with the
133 membrane via protein-protein interactions with Par-6 (Atwood et al., 2007; Petronczki and
134 Knoblich, 2001), the PS domain through direct interactions with lipids (Dong et al., 2020), and
135 the C1 which serves as a membrane targeting module in other PKCs (Colón-González and
136 Kazanietz, 2006), but has not been reported to do so in aPKCs. Removal of the C1 domain
137 from the regulatory domain (aPKC PB1-PS) leaving the PB1 and PS domains, resulted in a
138 protein that was not enriched at the membrane (Figure 4). Thus, the C1 domain is required for
139 membrane localization of the regulatory region – the PB1 and PS domains are not sufficient for
140 membrane targeting in NSCs. We next tested the C1 domain alone and found that it is
141 sufficient for uniform targeting to the membrane (Figure 4B-D). During interphase the C1
142 domain was bound to membrane but also highly nuclear enriched (Figure 4C). Thus, the aPKC
143 C1 domain is a membrane targeting module.

144 **C1 is a lipid binding module that is required for aPKC membrane recruitment**

145 How might the C1 domain mediate interaction with the NSC membrane? C1 domains in
146 canonical PKCs bind diacylglycerol, and although the aPKC C1 domain does not bind DAG
147 (Colón-González and Kazanietz, 2006), we sought to determine if it binds other phospholipids.
148 We used a vesicle pelleting assay in which Giant Unilamellar Vesicles (GUVs) with varying
149 phospholipid compositions were mixed with purified aPKC C1 domain. The vesicles were
150 separated from the soluble phase by ultracentrifugation and any associated C1 was identified
151 by protein gel electrophoresis. As shown in Figure 5A, we observed varying degrees of C1
152 binding to a broad array of phospholipids, suggesting that the C1 is a nonspecific phospholipid
153 binding module.

154 To better understand the role of the C1 in aPKC polarity, we examined the effect of removing it
155 (aPKC ΔC1) on aPKC's localization. As shown in Figure 4B-E, we found that aPKC ΔC1
156 remained in the cytoplasm, failing to bind the membrane. We conclude that the C1 is required
157 for aPKC membrane targeting in NSCs. Interestingly, Mira localization was also disrupted in

158 NSCs expressing aPKC ΔC1 suggesting that the C1 also plays a role in regulating aPKC's
159 protein kinase activity in NSCs. This observation is consistent with *in vitro* measurements of
160 kinase activity (Graybill et al., 2012; Zhang et al., 2014).

161 The PS domain has been reported to be a membrane binding module required for membrane
162 recruitment of aPKC in cultured cells and epithelia (Dong et al., 2020). Our results suggest that
163 the PS is not sufficient for localization to the NSC membrane (e.g. aPKC PB1-PS remains in the
164 cytoplasm). We tested whether the PS is required for NSC aPKC membrane recruitment by
165 examining the localization of aPKC in which the positively charged, basic residues were
166 removed and a negative charge added (aPKC AADAA). This mutation has been reported to
167 abrogate membrane binding in contexts where the PS is required (Dong et al., 2020). We found
168 that the apical localization of aPKC AADAA was only slightly reduced compared to WT aPKC
169 indicating that the PS is not required for aPKC's membrane recruitment or polarization in NSCs
170 (Figure 5B-E). Mira was cytoplasmic in NSCs expressing aPKC AADAA, however, indicating
171 that disrupting the PS activates kinase activity, consistent with the known function of the PS in
172 regulating catalytic activity (Graybill et al., 2012).

173 **Discussion**

174 The Par complex component aPKC undergoes a complex localization cycle in NSCs, targeting
175 to the apical membrane in mitosis and returning to the cytoplasm as division completes (Oon
176 and Prehoda, 2019). The function of interphase, cytoplasmic localization is unknown, but the
177 apical localization of aPKC during mitosis is necessary for the polarization of fate determinants
178 (Atwood et al., 2007; Prehoda, 2009; Rolls et al., 2003), a prerequisite for asymmetric cell
179 division. Regulated membrane recruitment of aPKC is a central aspect of Par-mediated polarity
180 and many physical interactions between aPKC and proteins and phospholipids have been
181 identified. Conceptually, targeting could occur through the concerted action of multiple weak
182 interactions (i.e., avidity). However, we discovered that the aPKC C1 domain is a phospholipid
183 binding module sufficient for membrane recruitment, whereas domains that mediate protein-
184 protein interactions or other interactions with phospholipids are not sufficient for aPKC
185 targeting. As the C1 is the only domain within aPKC with this capability in NSCs, our results
186 suggest that other aPKC domains, including the catalytic domain, function, at least in part, to
187 regulate the membrane recruitment activity of the C1. We propose that cooperative activation
188 of the C1 leads to the spatially and temporally controlled localization of aPKC observed in
189 many animal cells.

190 The C1 is unique in its ability to promote aPKC membrane recruitment in NSCs. While
191 numerous interactions between phospholipids and domains outside the C1 have been reported
192 (Wang et al., 2005; Ivey et al., 2014; Kajimoto et al., 2019; Dong et al., 2020), our results
193 indicate that they are not sufficient for membrane recruitment in NSCs. Similarly, the domains
194 that mediate protein-protein interactions, such as the PB1 that binds Par-6 and the PBM that
195 binds Baz, are also not sufficient for aPKC recruitment.

196 The constitutive nature of C1 membrane binding raises the question of how its activity is
197 regulated to yield aPKC's precisely controlled localization. The aPKC catalytic domain forms
198 intramolecular interactions with the PS and C1 that repress kinase activity (Graybill et al., 2012;
199 Lopez-Garcia et al., 2011; Zhang et al., 2014), forming an "inhibitory core" (Figure 5F). Our
200 results suggest the inhibitory core is coupled to C1 membrane binding. We observed C1
201 localization at the membrane throughout the cell cycle and uniform membrane binding in
202 mitosis when aPKC is normally restricted to the apical hemisphere. We also observed
203 constitutive membrane recruitment in aPKC variants where the catalytic domain was
204 perturbed, suggesting that it is required for repression of C1 activity. We suggest that
205 perturbations to the catalytic domain that influence protein kinase activity can also disrupt the
206 inhibitory core, consistent with the complex allosteric pathways in eukaryotic protein kinase
207 domains (Ahuja et al., 2019). It has been proposed that the PS plays a central role in
208 membrane recruitment and coupling localization to the inhibitory core through its interactions
209 with the catalytic domain (Dong et al., 2020). Our results indicate that the PS is not sufficient
210 for membrane recruitment, nor is its interaction with the aPKC catalytic domain required for
211 polarization in NSCs (aPKC AADAA is polarized but constitutively active). We conclude that, at
212 least in NSCs, the PS plays a more significant role in regulating catalytic activity than
213 localization.

214 Given that the C1 appears to be autoinhibited by the catalytic domain, how might it become
215 activated? We previously found that inactivation of the aPKC PBM (aPKC V606A), which binds
216 Baz, leads to cytoplasmic aPKC localization (Holly et al., 2020). Taken with our current results,
217 we suggest that the interaction with Baz is required for membrane recruitment not because
218 Baz directly recruits aPKC (e.g. aPKC ΔC1 is cytoplasmic), but because the Baz interaction is
219 required for disruption of the inhibitory core and activation of the C1. Similarly, in NSCs lacking
220 the PB1-binding Par-6 protein, aPKC also remains in the cytoplasm, even though Baz remains
221 properly polarized and could potentially bind aPKC's PBM. We propose that cooperative

222 activation of the C1 by at least Par-6 and Baz leads to the complex localization dynamics of
223 aPKC observed in NSCs. Future work will be directed at understanding how the aPKC PB1
224 and PBM might be coupled to the inhibitory core and activation of aPKC membrane binding.

225 **Materials and Methods**

226 *Drosophila*

227 Flies were grown at indicated temperatures on standard cornmeal/yeast media. Both male and
228 female larvae were used in this study. Transgenic constructs were cloned into the pUAST attB
229 vector (GenBank: EF362409.1) modified to include an N-terminal 3xHA or 1xHA tag. Integration
230 of the vectors was done using standard Phi-C31 integration into an attP landing site on the
231 third chromosome (attP2) by Rainbow Genetics or BestGene Inc. Positive insertion was
232 determined by the presence of colored eyes after backcrossing to y,w stock.
233

234 *Immunofluorescence*

235 For all overexpression crosses, *insc*-Gal4 virgins were crossed to males containing an aPKC
236 transgene on the third chromosome or an RNAi on the second chromosome and an aPKC
237 transgene on the third chromosome. Crosses laid in vials for 24 hours (~20˚C) for 24 hours. The
238 resulting embryos were incubated at 30˚C until larvae reached third instar wandering larva
239 stage. Following dissection, the tissue was incubated in 4% PFA fixative for 20' within 20' of
240 dissection. This and all subsequent wash steps involved agitation by placing on a nutator. After
241 fixation, brains were washed 1xquick, and 3x15' in PBST (1xPBS with 0.3% Triton-X). If brains
242 were not to be stained that day, they would then be placed at 4˚C for up to 3 days after which
243 a quick wash in PBST would be required before moving on to staining. If instead they were to
244 be stained, an additional wash step of 20' in PBST would occur. Brains were blocked for 30' in
245 PBSBT (PBST with 1% BSA) and then put into 1˚ overnight at 4˚C. The next day after removing
246 the 1˚, brains were washed 1xquick and 3x15' in PBSBT and put into 2˚ for 2 hours, protected
247 from light. After 2˚ was removed, brains were washed 1xquick and 3x15' in PBST. Brains were
248 stored in SlowFade w/DAPI at least overnight before imaging. Brains were imaged on an
249 upright confocal TCS SPE from Leica using an ACS APO 40x 1.15 NA Oil CS objective.

250 MARCM Immunofluorescence

251 To create MARCM larval NSC clones, FRT-G13, aPKC^{K06403}/CyO virgins were crossed with
252 3xHA aPKC D388A males. The subsequent progeny were allowed to grow to adulthood and

253 were screened for the absence of the CyO marker. Males with no CyO were then crossed to
254 elav-Gal4, UAS-mCD8:GFP, hs:flp; FRT-G13, tubPGal80 virgins.
255 Crosses laid in vials for 24 hours and the resulting embryos were incubated at room
256 temperature (~20˚C) for 24 hours. These vials were then heat shocked at 37˚C for 90 min.
257 Another heat shock was possible within 18 hours. Larvae were allowed to grow at room
258 temperature or 18˚C until third instar wandering larva stage, when they were dissected and
259 fixed as above.
260 *Membrane enrichment and polarization quantification*
261 Took measure of a 10px line through the central slice of a neuroblast from apical to basal
262 cortex. Apical was taken as the peak corresponding with the apical membrane and basal was
263 taken as the peak corresponding with the basal membrane. Where no peak was present, peaks
264 in other channels or the "edge" of signal before it dropped was used. Cytoplasmic signal was
265 taken as the average of 20 data points located 10 points from the apical peak.
266 All images were analyzed using Fiji and statistical analysis was done in Prizm.
267 All figures were put together using Adobe Illustrator.
268
269 *Lipid pulldown assay*
270 MBP-C1 was purified according to standard MBP purification protocols in our lab as previously
271 described (Graybill et al., 2012). For Giant Unilamellar Vesical (GUV) production, 50 µl of the
272 specified lipids at 10mg/mL in chloroform was dried in a test tube under an N_2 stream and then
273 in a vacuum chamber to ensure all chloroform was removed. Lipids were resuspended in a
274 0.2M sucrose solution to a final concentration of 0.5mg/mL and heated in a water bath at 50˚C
275 for 5 hours with occasional agitation. All lipids were stored at 4˚C and used within 3 days. For
276 this assay, 10X Dilution Buffer was made: 200mM HEPES, pH 7.5; 500mM NaCl, 10mM DTT.
277 All spins were carried out using an Optima MAX-TL Ultracentrifuge with a TLA-100 rotor at
278 65,000 at 4˚C.
279 MBP-C1 protein was diluted to 50µM in 1xDilution Buffer and pre-cleared for 30'. Reaction
280 conditions: 20mM HEPES, pH 7.5, 50mM NaCl, 1mM DTT, 0.25mg/mL GUVs, and 5µM MBP-
281 C1. Reaction was carried out at room temperature for 15' and then spun down for 30'. The
282 supernatant fraction was removed, and the pellet was resuspended in an equivalent volume of
283 1X Dilution buffer. Both the supernatant and pellet samples were mixed with 6x loading dye

284 and run on a 12.5% SDS-Page gel. Gels were stained with Coomassie and imaged using a
285 scanner.
286
287 **Key Resources Table**

Reagent type (species) or resource	Designation	Source or reference	Identifiers	Additional information
antibody	anti-aPKC	SCBT	Mouse Anti-PKC zeta (H1); SC-17781	1:1000
antibody	anti-Par-6	Alpha diagnostic	N/A	Rat Anti-Par-6 (polyclonal custom antibody); 1:500
antibody	anti-Mira	Abcam	Rat Anti-Mira; Ab197788	1:500
antibody	anti-HA	Cell Signaling Tech.	Rabbit Anti-HA (C29F4); 3724	1:1000
antibody	anti-HA	Covance	Mouse Anti-HA; MMS-101P	1:500
antibody	anti-Baz	C.Q.Doe Lab	N/A	Guinea Pig Anti-Baz (polyclonal custom antibody); 1:2000
antibody	anti-GFP	Abcam	Chicken Anti-GFP; Ab13970	1:500
antibody	anti-rat Cy3 secondary	Jackson Immuoresearch Lab.	Donkey Anti-Rat Cy3; 712-165-153	1:500
antibody	anti-rabbit 647 secondary	Jackson Immunoresearch Lab.	Donkey Anti-Rabbit 647; 711-605-152	1:500
antibody	anti-mouse 647 secondary	Jackson Immunoresearch Lab.	Donkey Anti-Mouse 647; 715-605-151	1:500
antibody	anti-mouse 488 secondary	Jackson Immunoresearch Lab.	Donkey Anti-Mouse 488; 715-545-151	1:500
antibody	anti-chicken 488 secondary	Jackson Immunoresearch Lab.	Donkey Anti-Chicken 488; 703-545-155	1:500
antibody	anti-guinea pig 405 secondary	Jackson Immunoresearch Lab.	Donkey Anti-Guinea Pig 405; 706-475-148	1:500
genetic reagent (*Drosophila melanogaster*)	*insc-GAL4*	Bloomington Drosophila Stock Center	*;insc-GAL4*	RRID:BDSC_8751

genetic reagent (*Drosophila melanogaster*)	*elav-GAL4*	Bloomington Drosophila Stock Center	*elav-Gal4, UAS-mCD8:GFP, hs:flp; FRT-G13, tubPGal80*	RRID:BDSC_5145
genetic reagent (*Drosophila melanogaster*)	*aPKC^{K06403}*	C.Q. Doe Lab	*; FRT-G13, aPKCK^{06403}/CyO*	
genetic reagent (*Drosophila melanogaster*)	HA-aPKC D388A	This study	;;3xHA-aPKC D388A (aPKC-PA)	
genetic reagent (*Drosophila melanogaster*)	HA-aPKC D388A	This study	;;1xHA-aPKC D388A (aPKC-PA)	
genetic reagent (*Drosophila melanogaster*)	HA-aPKC	This study	;;1xHA-aPKC 1-606 (aPKC-PA)	
genetic reagent (*Drosophila melanogaster*)	aPKC K293W	This study	;;1xHA-aPKC K293W (aPKC-PA)	
genetic reagent (*Drosophila melanogaster*)	aPKC PB1-C1	This study	;;1xHA-aPKC 1-195 (aPKC-PA)	
genetic reagent (*Drosophila melanogaster*)	aPKC PB1-PS	This study	;;1xHA-aPKC 1-141 (aPKC-PA)	
genetic reagent (*Drosophila melanogaster*)	aPKC C1	This study	;;1xHA-aPKC 139-195 (aPKC-PA)	
genetic reagent (*Drosophila melanogaster*)	aPKC ΔC1	This study	;;1xHA-aPKC 1-606 Δ141-196 (aPKC-PA)	
genetic reagent (*Drosophila melanogaster*)	aPKC AADAA	This study	;;1xHA-aPKC R131A, R132A, A134D, R135A, R136A (aPKC-PA)	
genetic reagent (*Drosophila melanogaster*)	Baz RNAi	Bloomington Drosophila Stock Center	*;UAS-Baz RNAi*	RRID:BDSC_39072
genetic reagent (*Drosophila melanogaster*)	Cdc42 RNAi	Bloomington Drosophila Stock Center	*;UAS-Cdc42 RNAi*	RRID:VDRC_100794
chemical compound, drug	Amylose Resin	NEB	E8021L	
chemical compound, drug	Schneider's Insect Medium (SIM)	Sigma	S0146	
chemical compound, drug	SlowFade Diamond Antifade Mountant with DAPI	Invitrogen	S36964	

chemical compound, drug	Phosphatidylserine (PS)	Avanti Polar Lipids	L-α-phosphatidylserine; 840032C	
chemical compound, drug	Phosphatidylcholine (PC)	Avanti Polar Lipids	L-α-phosphatidylcholine; 840051C	
chemical compound, drug	Phosphatidic acid (PA)	Avanti Polar Lipids	L-α-phosphatidic acid; 840101C	
chemical compound, drug	Phosphatidylglycerol (PG)	Avanti Polar Lipids	L-α-phosphatidylglycerol; 841138P	
chemical compound, drug	ceramide	Avanti Polar Lipids	C12 ceramide; 860512P	

References

Ahuja LG, Taylor SS, Kornev AP. 2019. Tuning the "violin" of protein kinases: The role of dynamics-based allostery. *IUBMB Life* **71**:685–696. doi:10.1002/iub.2057

Atwood SX, Chabu C, Penkert RR, Doe CQ, Prehoda KE. 2007. Cdc42 acts downstream of Bazooka to regulate neuroblast polarity through Par-6 aPKC. *J Cell Sci* **120**:3200–3206. doi:10.1242/jcs.014902

Atwood SX, Prehoda KE. 2009. aPKC phosphorylates Miranda to polarize fate determinants during neuroblast asymmetric cell division. *Curr Biol CB* **19**:723–729. doi:10.1016/j.cub.2009.03.056

Bailey MJ, Prehoda KE. 2015. Establishment of Par-Polarized Cortical Domains via Phosphoregulated Membrane Motifs. *Dev Cell* **35**:199–210. doi:10.1016/j.devcel.2015.09.016

Colón-González F, Kazanietz MG. 2006. C1 domains exposed: from diacylglycerol binding to protein-protein interactions. *Biochim Biophys Acta* **1761**:827–837. doi:10.1016/j.bbalip.2006.05.001

Dong W, Lu J, Zhang X, Wu Y, Lettieri K, Hammond GR, Hong Y. 2020. A polybasic domain in aPKC mediates Par6-dependent control of membrane targeting and kinase activity. *J Cell Biol* **219**:e201903031. doi:10.1083/jcb.201903031

Graybill C, Wee B, Atwood SX, Prehoda KE. 2012. Partitioning-defective protein 6 (Par-6) activates atypical protein kinase C (aPKC) by pseudosubstrate displacement. *J Biol Chem* **287**:21003–21011. doi:10.1074/jbc.M112.360495

Hannaford M, Loyer N, Tonelli F, Zoltner M, Januschke J. 2019. A chemical-genetics approach to study the role of atypical Protein Kinase C in Drosophila. *Dev Camb Engl* **146**:dev170589. doi:10.1242/dev.170589

Holly RW, Jones K, Prehoda KE. 2020. A Conserved PDZ-Binding Motif in aPKC Interacts with Par-3 and Mediates Cortical Polarity. *Curr Biol CB* **30**:893-898.e5. doi:10.1016/j.cub.2019.12.055

Homem CCF, Knoblich JA. 2012. Drosophila neuroblasts: a model for stem cell biology **139**:4297–4310. doi:10.1242/dev.080515

Ikeshima-Kataoka H, Skeath JB, Nabeshima Y, Doe CQ, Matsuzaki F. 1997. Miranda directs Prospero to a daughter cell during Drosophila asymmetric divisions. *Nature* **390**:625–629. doi:10.1038/37641

321 Ivey RA, Sajan MP, Farese RV. 2014. Requirements for pseudosubstrate arginine residues
322 during autoinhibition and phosphatidylinositol 3,4,5-$(PO_4)_3$-dependent activation of
323 atypical PKC. *J Biol Chem* **289**:25021–25030. doi:10.1074/jbc.M114.565671
324 Joberty G, Petersen C, Gao L, Macara IG. 2000. The cell-polarity protein Par6 links Par3 and
325 atypical protein kinase C to Cdc42. *Nat Cell Biol* **2**:531–539. doi:10.1038/35019573
326 Kajimoto T, Caliman AD, Tobias IS, Okada T, Pilo CA, Van A-AN, Andrew McCammon J,
327 Nakamura S-I, Newton AC. 2019. Activation of atypical protein kinase C by sphingosine
328 1-phosphate revealed by an aPKC-specific activity reporter. *Sci Signal* **12**:eaat6662.
329 doi:10.1126/scisignal.aat6662
330 Krahn MP, Klopfenstein DR, Fischer N, Wodarz A. 2010. Membrane targeting of Bazooka/PAR-
331 3 is mediated by direct binding to phosphoinositide lipids. *Curr Biol CB* **20**:636–642.
332 doi:10.1016/j.cub.2010.01.065
333 Lang CF, Munro E. 2017. The PAR proteins: from molecular circuits to dynamic self-stabilizing
334 cell polarity. *Dev Camb Engl* **144**:3405–3416. doi:10.1242/dev.139063
335 Lin D, Edwards AS, Fawcett JP, Mbamalu G, Scott JD, Pawson T. 2000. A mammalian PAR-3-
336 PAR-6 complex implicated in Cdc42/Rac1 and aPKC signalling and cell polarity. *Nat*
337 *Cell Biol* **2**:540–547. doi:10.1038/35019582
338 Lopez-Garcia LA, Schulze JO, Fröhner W, Zhang H, Süss E, Weber N, Navratil J, Amon S,
339 Hindie V, Zeuzem S, Jørgensen TJD, Alzari PM, Neimanis S, Engel M, Biondi RM. 2011.
340 Allosteric regulation of protein kinase PKCζ by the N-terminal C1 domain and small
341 compounds to the PIF-pocket. *Chem Biol* **18**:1463–1473.
342 doi:10.1016/j.chembiol.2011.08.010
343 Nance J, Zallen JA. 2011. Elaborating polarity: PAR proteins and the cytoskeleton. *Dev Camb*
344 *Engl* **138**:799–809. doi:10.1242/dev.053538
345 Oon CH, Prehoda KE. 2019. Asymmetric recruitment and actin-dependent cortical flows drive
346 the neuroblast polarity cycle. *eLife* **8**. doi:10.7554/eLife.45815
347 Petronczki M, Knoblich JA. 2001. DmPAR-6 directs epithelial polarity and asymmetric cell
348 division of neuroblasts in Drosophila. *Nat Cell Biol* **3**:43–49. doi:10.1038/35050550
349 Prehoda KE. 2009. Polarization of Drosophila neuroblasts during asymmetric division. *Cold*
350 *Spring Harb Perspect Biol* **1**:a001388. doi:10.1101/cshperspect.a001388
351 Rodriguez J, Peglion F, Martin J, Hubatsch L, Reich J, Hirani N, Gubieda AG, Roffey J,
352 Fernandes AR, St Johnston D, Ahringer J, Goehring NW. 2017. aPKC Cycles between
353 Functionally Distinct PAR Protein Assemblies to Drive Cell Polarity. *Dev Cell* **42**:400-
354 415.e9. doi:10.1016/j.devcel.2017.07.007
355 Rolls MM, Albertson R, Shih H-P, Lee C-Y, Doe CQ. 2003. Drosophila aPKC regulates cell
356 polarity and cell proliferation in neuroblasts and epithelia. *J Cell Biol* **163**:1089–1098.
357 doi:10.1083/jcb.200306079
358 Smith CA, Lau KM, Rahmani Z, Dho SE, Brothers G, She YM, Berry DM, Bonneil E, Thibault P,
359 Schweisguth F, Le Borgne R, McGlade CJ. 2007. aPKC-mediated phosphorylation
360 regulates asymmetric membrane localization of the cell fate determinant Numb. *EMBO*
361 *J* **26**:468–480. doi:10.1038/sj.emboj.7601495
362 Standaert ML, Galloway L, Karnam P, Bandyopadhyay G, Moscat J, Farese RV. 1997. Protein
363 kinase C-zeta as a downstream effector of phosphatidylinositol 3-kinase during insulin
364 stimulation in rat adipocytes. Potential role in glucose transport **272**:30075–30082.
365 Tepass U. 2012. The Apical Polarity Protein Network in Drosophila Epithelial Cells: Regulation
366 of Polarity, Junctions, Morphogenesis, Cell Growth, and Survival **28**:655–685.
367 doi:10.1146/annurev-cellbio-092910-154033

368 Venkei ZG, Yamashita YM. 2018. Emerging mechanisms of asymmetric stem cell division. *J*
369 *Cell Biol*. doi:10.1083/jcb.201807037
370 Wang G, Silva J, Krishnamurthy K, Tran E, Condie BG, Bieberich E. 2005. Direct binding to
371 ceramide activates protein kinase Czeta before the formation of a pro-apoptotic
372 complex with PAR-4 in differentiating stem cells. *J Biol Chem* **280**:26415–26424.
373 doi:10.1074/jbc.M501492200
374 Wodarz A, Ramrath A, Grimm A, Knust E. 2000. Drosophila atypical protein kinase C
375 associates with Bazooka and controls polarity of epithelia and neuroblasts. *J Cell Biol*
376 **150**:1361–1374. doi:10.1083/jcb.150.6.1361
377 Zhang H, Neimanis S, Lopez-Garcia LA, Arencibia JM, Amon S, Stroba A, Zeuzem S, Proschak
378 E, Stark H, Bauer AF, Busschots K, Jørgensen TJD, Engel M, Schulze JO, Biondi RM.
379 2014. Molecular mechanism of regulation of the atypical protein kinase C by N-terminal
380 domains and an allosteric small compound. *Chem Biol* **21**:754–765.
381 doi:10.1016/j.chembiol.2014.04.007
382

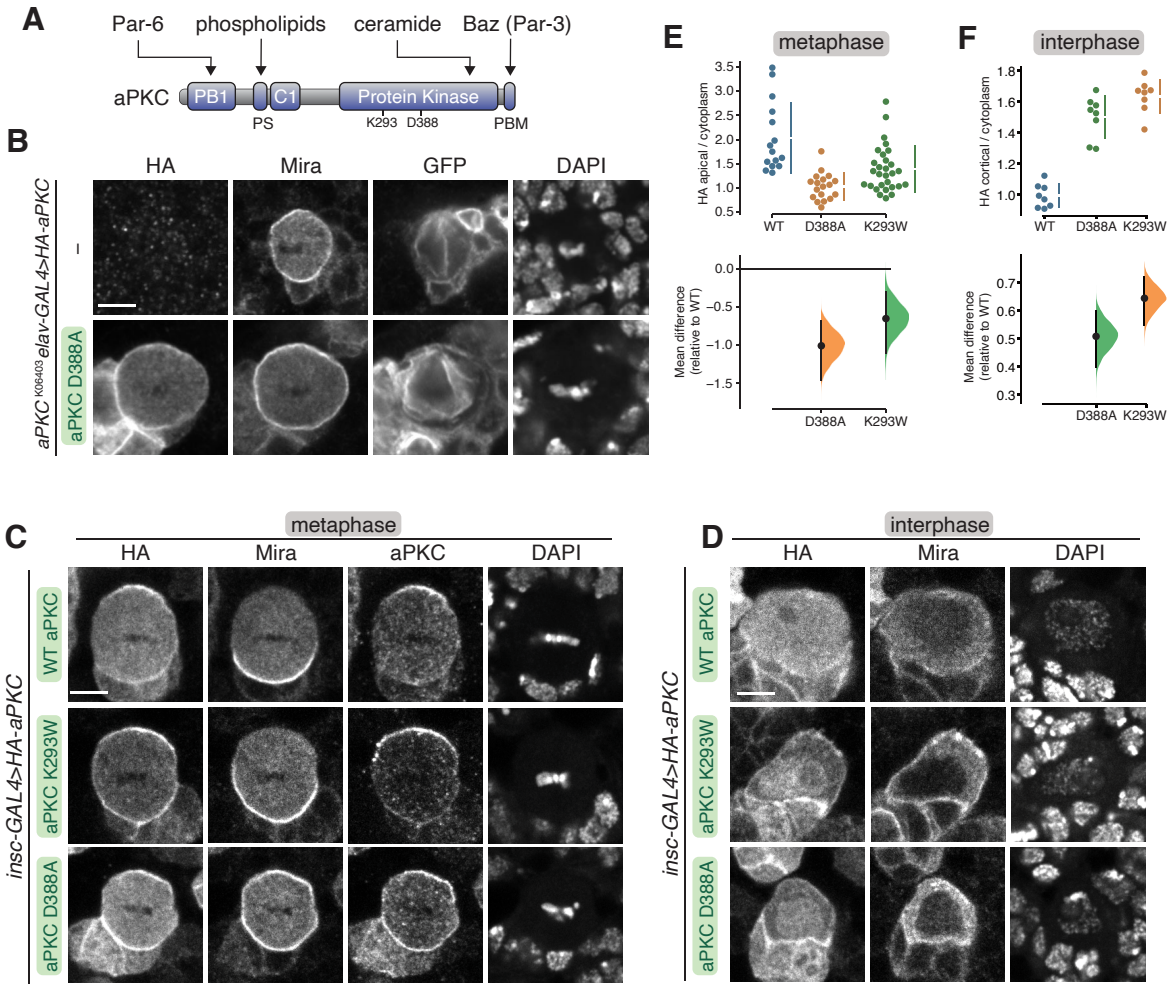

Figure 1 Localization of aPKC with kinase inactivating mutations in larval brain NSCs

(A) Domain structure of aPKC showing the location of PB1, PS (pseudosubstrate), C1, kinase domains, PBM (PDZ binding motif), along with location of K293 and D388 residues.

(B) Localization of HA tagged aPKC harboring the D388A kinase inactivating mutation in a metaphase, positively marked (mCD8-GFP) *aPKC*^{K06403} mutant larval brain NSC. Expression of D388A was driven by UAS and elav-GAL4. An *aPKC*^{K06403} mutant larval brain NSC is shown for comparison. Nucleic acids are shown with DAPI. Scale bar is 5 μm in all panels.

(C) Localization of HA tagged aPKC harboring either the D388A or K293W kinase inactivation mutations in metaphase larval brain NSCs with endogenous aPKC. The basal cortical marker Miranda, total aPKC ("aPKC", endogenous and exogenously expressed), and nucleic acid (DAPI) are also shown.

(D) Localization of HA tagged aPKC harboring either the D388A or K293W kinase inactivation mutations in interphase larval brain NSCs with endogenous aPKC. The basal cortical marker Miranda and nucleic acid (DAPI) are also shown.

(E) Gardner-Altman estimation plot of the effect of the D388A and K293W mutations on metaphase aPKC membrane recruitment. Apical cortical to cytoplasmic signal intensities of anti-HA signals are shown for individual metaphase NSCs expressing either HA-WT or HA-D388A or HA-K293W aPKC. Statistics: bootstrap 95% confidence interval (bar in “D388A” and “K293W” column).

(F) Gardner-Altman estimation plot of the effect of the D388A and K293W mutations on interphase aPKC membrane recruitment. Cortical to cytoplasmic cortical signal intensities of anti-HA signals are shown for individual metaphase NSCs expressing either HA-WT or HA-D388A or HA-K293W aPKC. Statistics: bootstrap 95% confidence interval (bar in “D388A” and “K293W” column).

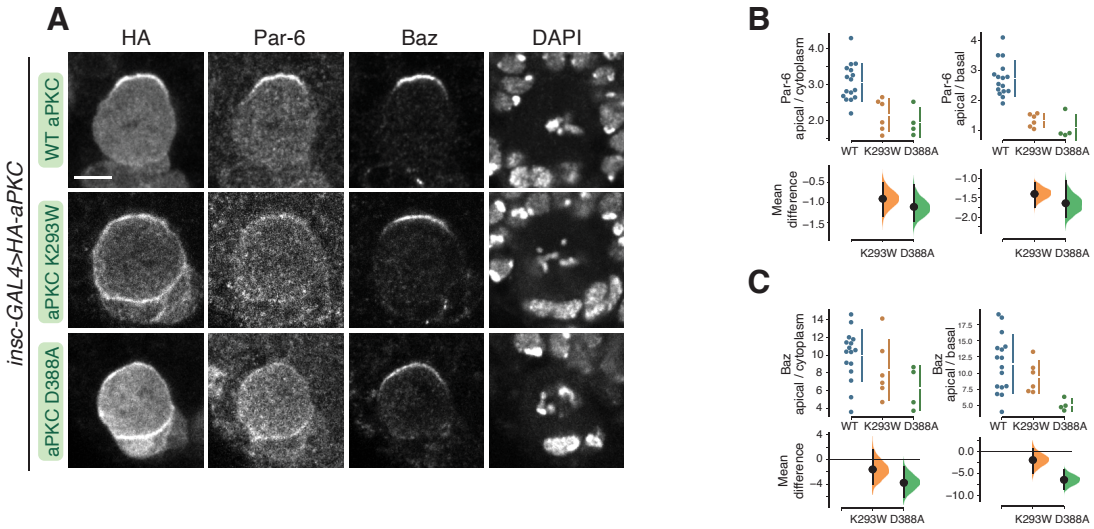

Figure 2 Localization of Bazooka and Par-6 in larval brain NSCs expressing kinase inactive aPKCs
(A) Localization of Par-6 and Bazooka (Baz) in metaphase larval brain NSCs expressing HA tagged aPKC D388A or aPKC K293W via UAS and insc-GAL4. Nucleic acids are shown with DAPI. Scale bar is 5 μm.
(B) Gardner-Altman estimation plots of the effect of expressing aPKC D388A or aPKC K293W on Par-6 cortical localization and polarity. Apical cortical to cytoplasmic or basal cortical signal intensities of anti-Par-6 signals are shown for individual metaphase NSCs expressing either HA-WT or HA-D388A or HA-K293W aPKC. Statistics: bootstrap 95% confidence interval (bar in "D388A" and "K293W" column).
(C) Gardner-Altman estimation plots of the effect of expressing aPKC D388A or aPKC K293W on Baz cortical localization and polarity. Apical cortical to cytoplasmic or basal cortical signal intensities of anti-Baz signals are shown for individual metaphase NSCs expressing either HA-WT or HA-D388A or HA-K293W aPKC. Statistics: bootstrap 95% confidence interval (bar in "D388A" and "K293W" column).

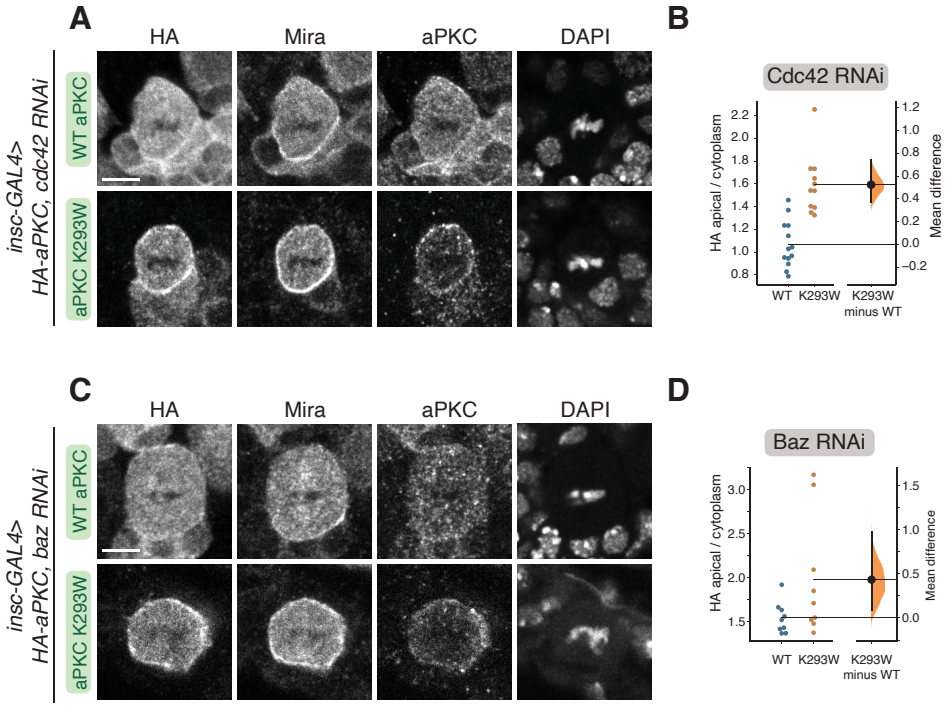

Figure 3 Cortical localization of kinase inactive aPKC in NSCs lacking Bazooka or Cdc42
(A) Localization of HA tagged aPKC K293W in metaphase larval brain NSCs expressing an RNAi directed against Cdc42. Scale bar is 5 μm in all panels.
(B) Gardner-Altman estimation plots of the effect of expressing Cdc42 RNAi on WT and K293W aPKC cortical localization. Apical cortical to cytoplasmic signal intensities of anti-HA signals are shown for individual metaphase NSCs expressing either HA-WT or HA-K293W aPKC. Statistics: bootstrap 95% confidence interval.
(C) Localization of HA tagged aPKC K293W in metaphase larval brain NSCs expressing an RNAi directed against Bazooka.
(D) Gardner-Altman estimation plots of the effect of expressing Baz RNAi on WT and K293W aPKC cortical localization. Apical cortical to cytoplasmic signal intensities of anti-HA signals are shown for individual metaphase NSCs expressing either HA-WT or HA-K293W aPKC. Statistics: bootstrap 95% confidence interval.

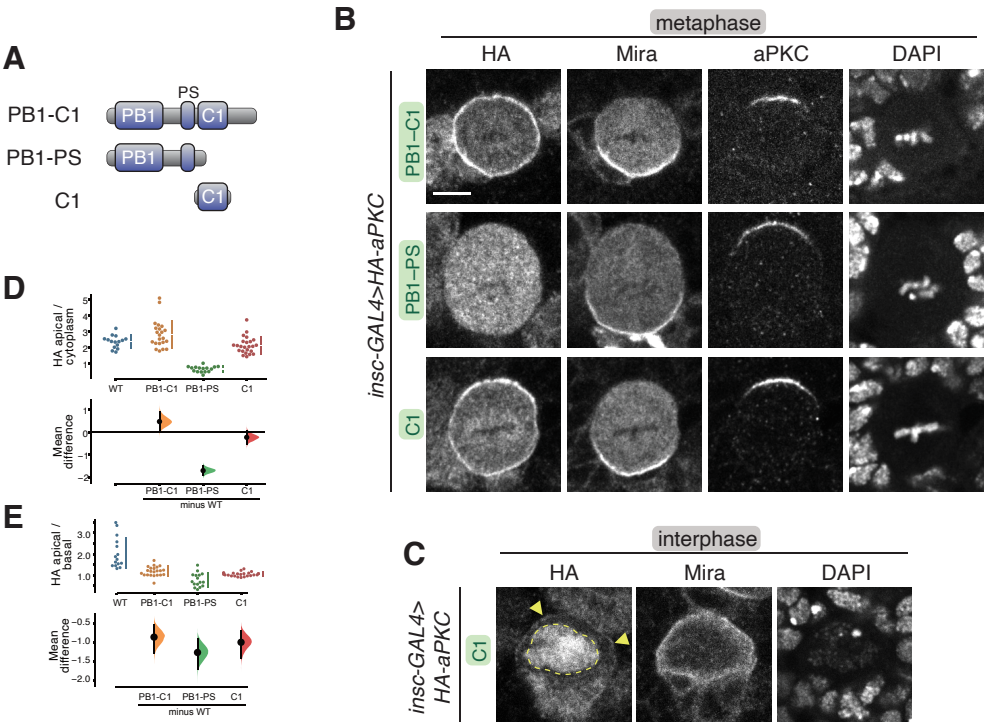

Figure 4 Localization of the aPKC regulatory domain variants in larval brain NSCs
(A) Schematics of regulatory domain variants of aPKC.
(B) Localization of HA tagged aPKC regulatory domain variants in metaphase larval brain NSCs. The basal marker Miranda, endogenous aPKC (using an antibody that does not react with the regulatory domain), nucleic acids (DAPI) are shown for comparison. Scale bar is 5 μm.
(C) Localization of the HA tagged aPKC C1 domain in interphase larval brain NSCs. Arrowheads highlight the membrane signal and the nuclear signal is outlined by a dashed line.
(D) Gardner-Altman estimation plot of aPKC regulatory domain cortical localization. Apical cortical to cytoplasmic signal intensity ratios of anti-HA signals are shown for individual metaphase NSCs expressing either aPKC PB1-C1 or PB1-PS or C1 regulatory domain fragments. Statistics: bootstrap 95% confidence interval.
(E) Gardner-Altman estimation plot of aPKC regulatory domain polarity. Apical cortical to basal cortical signal intensity ratios of anti-HA signals are shown for individual metaphase NSCs expressing either aPKC PB1-C1 or PB1-PS or C1 regulatory domain fragments. Statistics: bootstrap 95% confidence interval.

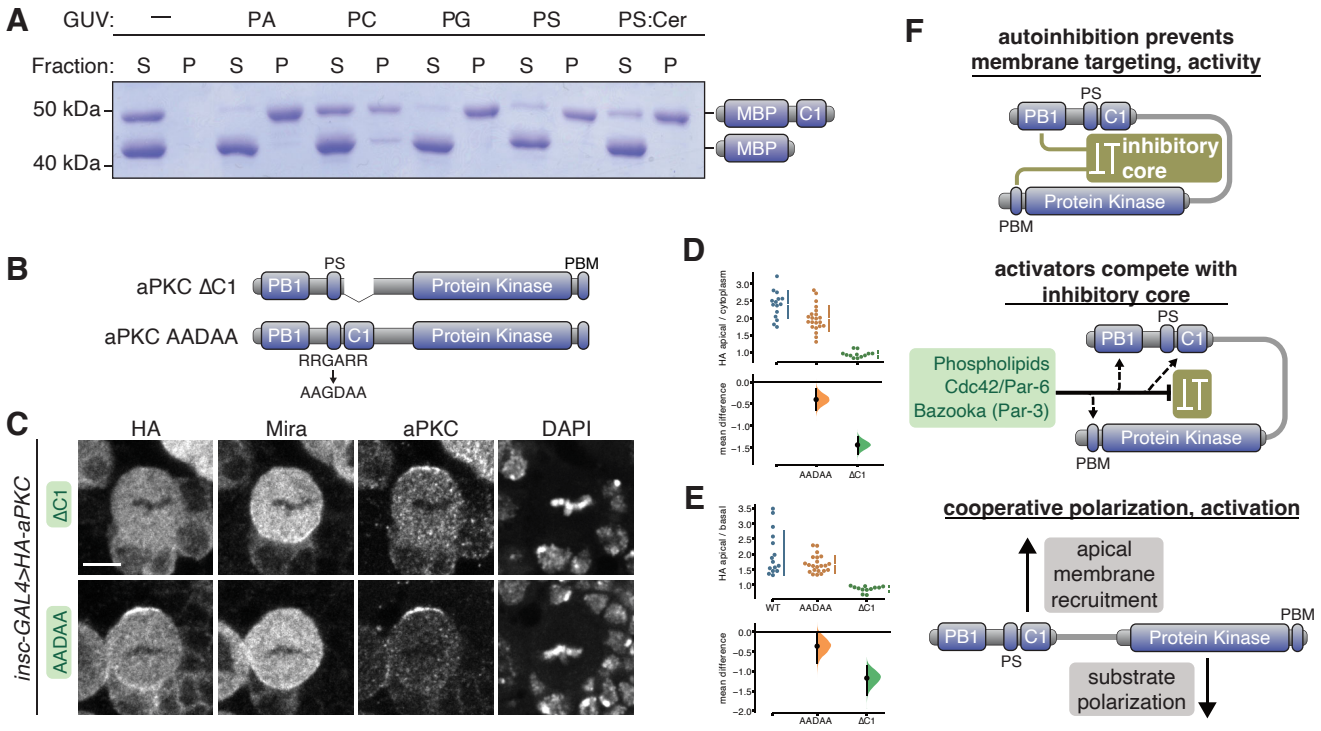

Figure 5 The aPKC C1 domain is a cortical localization module that is required for aPKC polarity
(A) Binding of a maltose binding protein (MBP) fusion of the aPKC C1 domain to phospholipids. Supernatant (S) and pellet (P) fractions from cosedimentation with Giant Unilamellar Vesicles (GUVs) of the indicated phospholipid composition are shown (PA, phosphatidic acid; PC, phosphatidyl choline; PG, phosphatidyl glycerol; PS, phosphatidyl serine; PS:Cer, phosphatidyl serine mixture with ceramide). MBP alone is included as an internal negative control.
(B) Schematics of ΔC1 and AADAA aPKC variants.
(C) Localization of HA tagged aPKC ΔC1 and AADAA variants in metaphase larval brain NSCs. The basal marker Miranda, total aPKC (expressed variant and endogenous), nucleic acids (DAPI) are shown for comparison. Scale bar is 5 μm.
(D) Gardner-Altman estimation plot of aPKC AADAA and ΔC1 cortical localization. Apical cortical to cytoplasmic signal intensity ratios of anti-HA signals are shown for individual metaphase NSCs expressing either aPKC AADAA or ΔC1. Statistics: bootstrap 95% confidence interval.
(E) Gardner-Altman estimation plot of aPKC AADAA and ΔC1 polarization. Apical cortical to basal cortical signal intensity ratios of anti-HA signals are shown for individual metaphase NSCs expressing either aPKC AADAA or ΔC1. Statistics: bootstrap 95% confidence interval.
(F) Model for cooperative polarization and activation of aPKC. An inhibitory core couples repression of catalytic activity (protein kinase domain) to membrane localization (C1 with some contribtion from PS). The PB1 and PBM are also coupled to the inhibitory core to allow for cooperative activation by Cdc42/Par-6 binding to the PB1 and Baz binding to the PBM. Disruption of the inhibitory core leads to spatially (apical) and temporally (mitotic) regulated localization and activation of catalytic activity.